energy&fuels

Article

pubs.acs.org/EF

Behavior of Inorganic Matter in a Dual Fluidized Steam Gasification Plant

Friedrich Kirnbauer,*[,†] Markus Koch,[‡] Reinhard Koch,[‡] Christian Aichernig,[§] and Hermann Hofbauer[∥]

[†]Bioenergy 2020+ GmbH, Wiener Straße 49, A-7540 Güssing, Austria

[‡]Biomasse-Kraftwerk Güssing GmbH, Europastraße 1, A-7540 Güssing, Austria

[§]Repotec Umwelttechnik GmbH, Europastraße 1, A-7540 Güssing, Austria

[∥]Vienna University of Technology, Institute of Chemical Engineering, Getreidemarkt 9/166, 1060 Vienna, Austria

ABSTRACT: Ash components of biomass fuels can cause fouling, slagging, and bed material agglomeration during thermal utilization in fluidized bed combustion and gasification plants. The influence of ash components on these problems in dual fluidized bed biomass gasification plants is investigated in an industrial scale plant in Güssing, Austria. Samples of fouling are analyzed, and the results are evaluated. The samples were analyzed by X-ray fluorescence analysis and thermal analyses such as thermogravimetric analysis, differential thermal analysis, and differential scanning calorimetry. Mass balances of inorganic matter are presented, evaluating different loop configurations. The analyses showed high potassium contents compared to the fuel ash composition in fouling of up to 23% by weight. The potassium content of fly ash with a particle size smaller than 200 μm is half that of coarse fly ash with a particle size larger than 200 μm. The thermal analyses showed a large difference between samples of inorganic streams such as fly ash or fly char and fouling. Different fractions of fly ash samples (particle fraction smaller than 200 μm and particle fraction larger than 200 μm) showed similar thermal behavior: endothermic weight losses at around 400 °C and around 720−820 °C caused by decomposition of carbonates. The composition of inorganic matters of fly ash and fly char is similar. The elemental composition of deposits at the cyclone wall and the first heat exchanger in the flue gas path showed high potassium contents up to 23.6%. While samples of fly ash and fly char did not show significant melting in their thermal behavior, melting could be detected with fouling at temperatures higher than 1000 °C. Mass balances of inorganic matter showed a flow of potassium oxide from the combustion reactor to the gasification reactor, which leads to unexpected high potassium concentrations in the fly char. A reduction of ash loops reduces the amount of potassium that is transferred from the combustion reactor to the gasification reactor. Recommendations are made for the operation of dual fluidized bed gasification plants in terms of ash handling to reduce tendencies for fouling, slagging, and bed material agglomeration.

INTRODUCTION

Biomass fuels are well-known to cause operational problems and unscheduled downtime in fluidized bed combustion plants. These problems are often caused by slagging, fouling, and bed material agglomeration.[1,2] Gasification plants face similar problems. Studies published about fouling, slagging, and bed material agglomeration in gasification plants are often carried out in lab-scale test rigs, but studies of these phenomena in industrial-scale gasification plants are sparse. This might be due to a lack of operating fluidized bed biomass gasification plants.[3]

A technology for the gasification of biomass, which is demonstrated successfully at industrial scale, is biomass steam gasification in a dual fluidized bed (DFB) gasifier. Various plants working with the DFB gasification technology are in operation, for example, in Güssing (Austria; 8 MWth),[4] Oberwart (Austria; 8.5 MWth),[5] Villach (Austria; 15 MWth),[6] and Ulm (Germany; 15.1 MWth).[7]

The DFB biomass steam gasification plant in Güssing was the first industrial scale DFB biomass steam gasification plant to go into operation. It began operating in 2002 and demonstrated the DFB process successfully.

Because this plant in Güssing was the first installation of an industrial-scale DFB steam gasification plant, potential for improvements in terms of plant design and engineering was determined. These disadvantages in the design of the Güssing plant lead to a higher risk of fouling and slagging. Knowledge about design improvements was considered in plants that were constructed recently, and fouling and slagging cannot be determined in the gasification plant in Oberwart, for example. The present operation of the plant in Güssing also differs from what was defined during the planning phase in some aspects.

The fuel−water content has a big influence on the operation, and is 33% on average today; in comparison, the design value was 15%. The consequence is that the combustion chamber is operated with a higher load than designed, which leads to higher velocities and lower excess air.

However, a better understanding of the fouling and slagging mechanism for woody biomass at the plant in Güssing may be a precondition for design improvements in future plants and for the utilization of cheaper alternative fuels in DFB gasifiers such as energy crops, straw, sewage sludge, and so on. By now, the gasification plants are running with woody biomass as a fuel.

This study is part of a process of overall optimization of the plant to increase its efficiency in terms of technological efficiency, economic efficiency, and availability. This paper presents the results of analyses of inorganic matter in solid flow streams and

Received: April 5, 2013
Revised: May 23, 2013
Published: May 29, 2013

   dx.doi.org/10.1021/ef400598h | *Energy Fuels* 2013, 27, 3316−3331

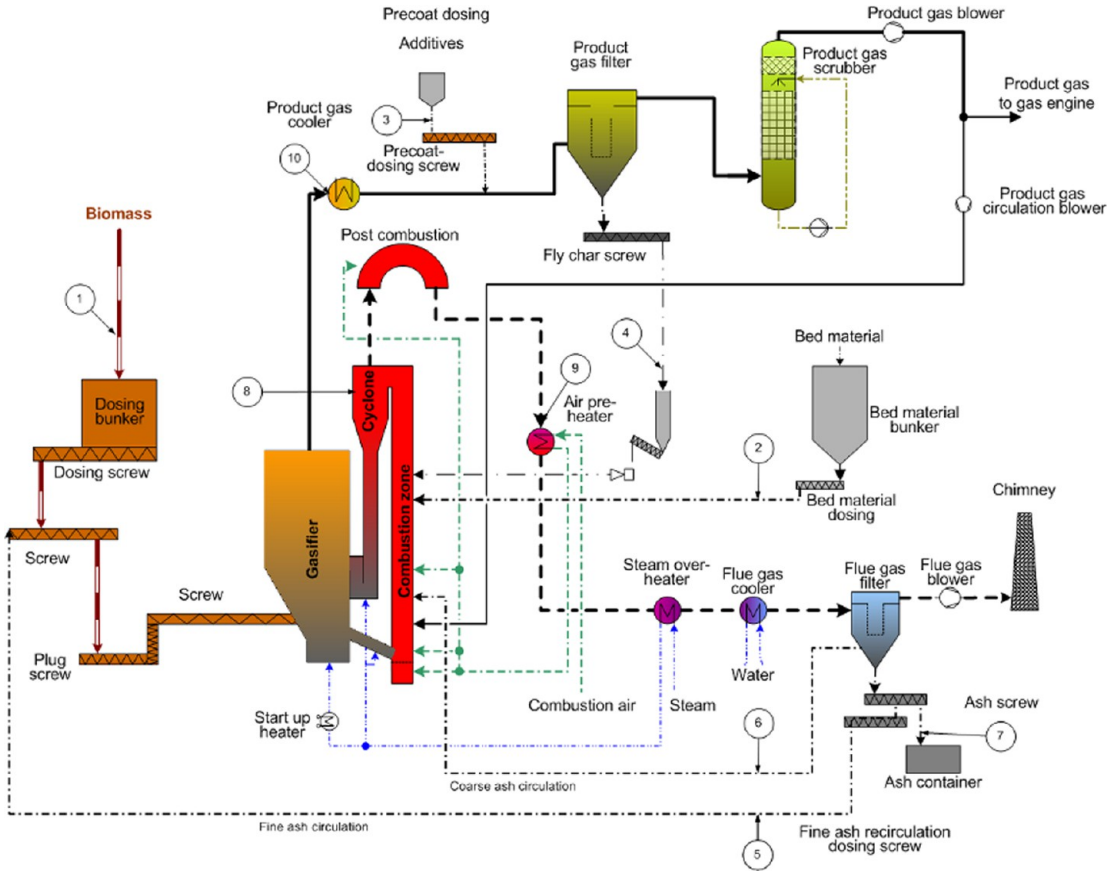

Figure 1. Flow sheet of the CHP plant in Güssing with sampling points.

fouling and documents different ash loop setups with balances of inorganic matter at the plant in Güssing. The formation mechanism of fouling is investigated, and suggestions for a mechanism are given. Proposals for improvements of the inorganic loops and the operation of the plant are given.

FUNDAMENTALS

The principle of DFB steam gasification is based on the separation of the endothermic gasification process and the external heat supply from a separate combustion chamber. Heat is transferred via circulating bed material between the gasification zone (gasifier) operated in bubbling bed mode and the combustion reactor operated in fast-fluidized bed mode. Details of the DFB steam gasification process are summarized elsewhere.[4,8−13] A basic flow sheet of the Güssing plant with a focus on inorganic material streams is shown in Figure 1.

Input streams for inorganic matter are biomass streams into the gasifier (wood chips), precoat material (dolomite) prior to the product gas filter, and bed material supplement to the combustion zone. The output stream is only fly ash that leaves the process after the flue gas filter and is collected in a container.

The main internal stream of inorganic matter is the circulation stream of bed material between the gasifier and the combustion zone. A fine fraction of inorganic matter such as biomass ash and abraded bed material leaves the gasifier with the product gas and is separated in the product gas filter (fly char). This dust from the product gas filter contains organic matter that is not gasified, such as char and tar. To utilize this remaining energy, char and tars are burned in the combustion zone.

Inorganic matter plays an important role in the gasification properties but can also lead to fouling, slagging, and bed material agglomeration, which can cause unplanned shutdowns of thermal biomass conversion plants. Various studies of fouling and bed agglomeration are available in the literature, with a focus on the utilization of coal with biomass,[14−16] but several studies are also available for woody or other biomass combustion.[2,17−20] The difference between combustion plants and the DFB biomass gasifier in terms of fouling, slagging, and bed agglomeration is caused by the utilization of two main reactors: a gasification reactor with a reducing atmosphere and a combustion reactor with an oxidizing atmosphere. Intensive exchange of inorganic matters originating from the fuel and bed materials occurs between the two reactors. In contrast to regular fluidized bed combustion plants where quartz sand is used, the bed material in DFB biomass gasification plants is olivine, which is a magnesium iron silicate.

Ash of woody biomass can be described as a system that is dominated by silicates with different contents of basic oxides and a high content of volatile alkaline sulfates and alkaline chlorides.[21,22] Besides alkali metals, the alkali earth metals also react to form silicates.[21,22]

The state of matter of the inorganic material (solid, liquid, gas) plays an important role in the reactivity of the substances. Table 1 shows general relationships of the state of matter and the reactivity of the substances. Two gaseous components show the highest reactivity, followed by a gaseous and a liquid component. Gaseous and solid components have a higher reactivity than two liquid components, followed by a liquid and a solid component. Two solid components show the lowest

dx.doi.org/10.1021/ef400598h | Energy Fuels 2013, 27, 3316−3331

Table 1. Influence of the Physical Form of the Substances on the Reactivity[21]

reactivity of the ash[a]	
(g) + (g) ≫ (g) + (l) > (g) + (s) > (l) + (l) > (l) + (s) ≫ (s) + (s)	equation 1

[a](g) gaseous elements, (l) liquid elements, (s) solid elements.

reactivity with each other. This is valid for the reactivity and the reaction rate.[22]

The substances that are typically detectable in biomass ashes can be split into acid and basic substances (Table 2). The reactivity decreases from the first to the last row.[22]

Table 2. Classification of Ash Compounds[22]

basic cmpds	acidic cmpds
KOH (l, g) (K_2O)	P_2O_5 (g)
NaOH (l, g) (Na_2O)	SO_2 (g)/SO_3 (g)
CaO (s)	SiO_2 (s)
MgO (s)	HCl (g) (Cl_2)
H_2O (g)	CO_2
	H_2O (g)

Considering the main components of biomass ash, a binary mixture of potassium and silicon oxides is the substance with the lowest melting point, forming a eutectic point at 752 °C with a ratio of 31% K_2O to 69% SiO_2 by weight. Three different crystal phases are formed: $K_2O{\cdot}SiO_2$ (melting point 976 °C), $K_2O{\cdot}2SiO_2$ (melting point 1036 °C), and $K_2O{\cdot}4SiO_2$ (melting point 765 °C).[23]

The phase diagram for the three-component system of the oxides of potassium, calcium, and silicon, which represents the main components of biomass ash, forms eutectic points with melting temperatures of around 850 °C.[24] Other elements such as sulfur, chlorine, and potassium have a significant influence on the physical form of the ash mixture at high temperature. The main reactions of ash components were summarized by Boström et al.[22] and are shown in Table 3. These reactions can take place under proper conditions such as temperature, pressure, and availability of reaction partners. Mineral substances can be formed, and amorphous melts can also be detected at fast cooling rates.

The release of alkaline metals in the gas phase is important for the formation of fouling, slagging, and bed material agglomeration because these elements condense after cooling and react with other elements during condensation, which can lead to fouling at heat exchangers. On the other hand, the reactivity of elements in the gas phase is higher compared to elements incorporated in a solid crystal structure, as described above.

Van Lith et al.[25] studied the mechanism and modification of potassium during the devolatilization and combustion of biomass, as shown in Figure 2. Due to its metabolic function, potassium is highly mobile within all levels of the plant. During drying of the wood, potassium is likely to precipitate in the form of salts such as KCl, K_2SO_4, KOH, and K_2CO_3. Some of the potassium is bound in organic structures in carboxyl groups. In spruce and beech, about 40% of the potassium is organically associated. During devolatilization and combustion of biomass, organically bound potassium and inorganic bound potassium follow different reaction schemes. Inorganic bound potassium (e.g., potassium chlorine) is stable and is evaporated at higher temperatures. Carboxyl groups start to decompose at temperatures lower than 300 °C, and atomic potassium will be released. This elemental potassium is likely to react with phenol groups, which are stable at these temperatures, or it remains in the gas phase. At higher temperatures, it is suggested that potassium is bound to phenol groups, which decompose at temperatures higher than 400 °C, while potassium is released to the gas phase, probably in elemental form. During the combustion at temperatures about 850 °C, organically bound potassium is oxidized to potassium carbonate. Elemental potassium can also react with minerals that remain stable, or it reacts with oxygen to form potassium carbonate. The decomposition of potassium carbonate (K_2CO_3) seems to be the dominant mechanism at temperatures higher than 800 °C.

Novaković et al.[26] showed in laboratory scale trials with mixtures of potassium, calcium, and silicon that the release of potassium into the gas phase is mainly dependent on the calcium content in the mixture, the water content in the gas phase, and the temperature. The release rate is independent of the origin of the calcium (e.g., $CaCO_3$ or $Ca(OH)_2$). The absence of steam reduces the release of potassium, while doubling the calcium content brings a higher release of potassium.

Table 3. Survey of Major Secondary Ash-Forming Reactions (Schematic)[22]

reaction	comments	
$P_2O_5(g) + 2KOH(g) \leftrightarrow 2KPO_3(l, g) + H_2O(g)$	fast reaction,[a] product molten and partially volatile in residual ash[b]	equation 2
$SO_3(g) + 2KOH(g) \leftrightarrow K_2SO_4(l, g) + H_2O(g)$	fast reaction, product molten or not	equation 3
$HCl(g) + KOH(g) \leftrightarrow KCl(g, l) + H_2O(g)$	fast reaction, product not stable in residual ash	equation 4
$SiO_2(s) + 2KOH(g) \leftrightarrow K_2SiO_3(l) + H_2O(g)$	medium fast reaction, product stable and molten in residual ash	equation 5
$CO_2(g) + 2KOH(g) \leftrightarrow K_2CO_3(l, g) + H_2O(g)$	fast reaction, product not stable in residual ash	equation 6
$P_2O_5(s) + 3CaO(s) \leftrightarrow Ca_3P_2O_8(s)$	medium fast reaction, product stable and solid in residual ash	equation 7
$SO_3(g) + CaO(s) \leftrightarrow CaSO_4(s, l)$	medium fast reaction, product (not) stable and solid in residual ash	equation 8
$2HCl(g) + CaO(s) \leftrightarrow CaCl_2(g, l) + H_2O(g)$	medium fast reaction, product not stable in residual ash	equation 9
$SiO_2(s) + CaO(s) \leftrightarrow CaSiO_3(s)$	slow reaction,[c] product stable and solid in residual ash	equation 10
$CO_2(g) + CaO(s) \leftrightarrow CaCO_3(s)$	medium fast reaction, product not stable in residual ash[b]	equation 11
$K_2SiO_3(l) + CaO(s) \leftrightarrow K - Ca - Silicate(l)$	rather slow reaction,[c] product stable and molten in residual ash	equation 12

[a]The reaction rates are classified into four categories on an arbitrary scale. [b]The stability in residual ash varies according to the thermal condition of the specific appliance. [c]These reaction rates are also highly dependent upon the dispersion of fuel and reactant particles.

dx.doi.org/10.1021/ef400598h | Energy Fuels 2013, 27, 3316−3331

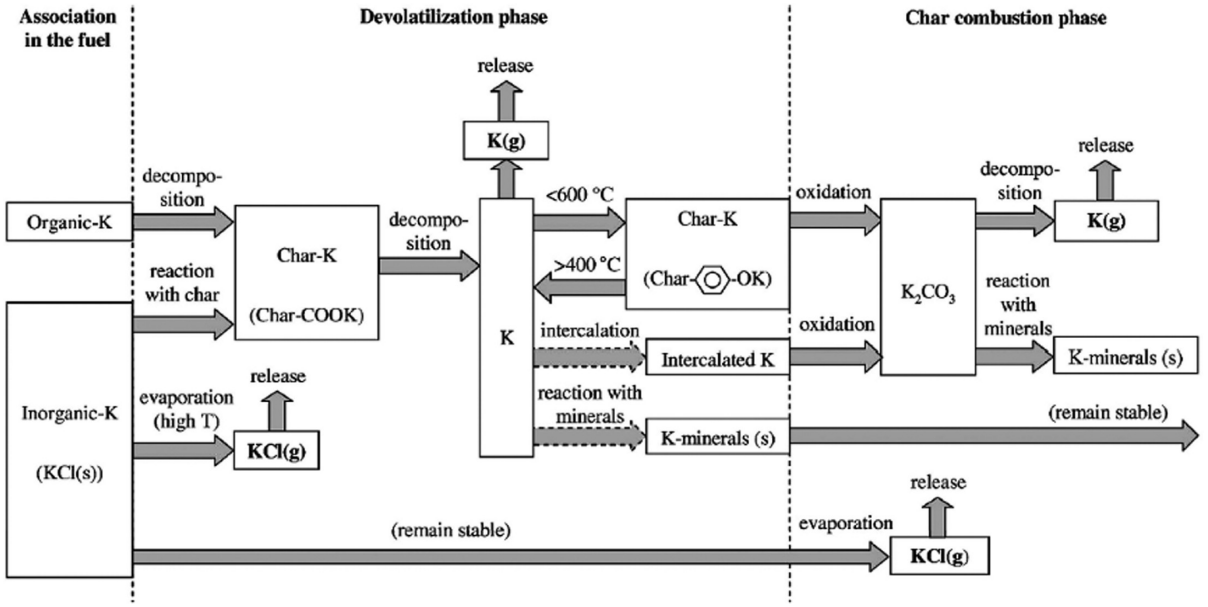

Figure 2. Possible transformations and release mechanisms of organically associated K and KCl during devolatilization and combustion of biomass.[25]

The chemical mechanism of the release of potassium from potassium carbonate is shown in eq 6. An excess of water moves the equilibrium according to Le Chatelier's principle toward KOH(g) and CO_2(g) and, with that, toward a higher release rate of potassium into the gas phase.

Comparing the release of potassium into the gas phase in an oxidizing atmosphere (combustion) and a reducing atmosphere (gasification), a higher release rate can be expected in the reducing atmosphere of the gasification reactor at the same temperatures.[27,28]

The consequences of ash melting or the release of inorganic matter into the gas phase can be fouling, slagging, and bed material agglomeration. Deposits occurring in the high temperature sections of furnaces are called slagging. Radiative heat transfer is dominant in the areas where slagging occurs. Deposits in the convective heat transfer zones of the boiler are called fouling and take place in the areas where the gases are cooled.[16]

The interaction of biomass ash with the bed material of the fluidized bed can lead to bed material agglomeration. Bed material agglomeration cannot be seen in DFB biomass steam gasification plants because olivine is used as a bed material, which has a lower agglomeration tendency compared to silicon sand.[29]

Earlier studies showed that the bed material olivine is modified during utilization in the plant.[10] Two different calcium-rich layers are formed at the surface of the bed material particles. The inner layer is homogeneous and consists mainly of calcium and silicate. The outer layer has a similar composition to the fly ash.

The importance of this calcium-rich layer concerning the gasification properties was shown in two earlier studies at a 100 kW pilot plant at the Vienna University of Technology.[11,12] The water−gas shift reaction is enhanced, leading to higher hydrogen and CO_2 contents in the product gas and to a lower carbon monoxide content and a lower content of higher hydrocarbons. The decomposition of primary tars is enhanced, and the formation of secondary tars is reduced, leading to lower total tar concentrations in the product gas.

Detailed investigations on the mechanism of the layer formation at the bed material were presented by Kirnbauer et al.[30] Investigations of the composition of the surface of used bed material in gasification and combustion atmosphere did not show a change in the elemental composition but showed a slight change in the crystal structure. Thermal investigations show a weak endothermic weight loss with used bed material in CO_2-rich atmosphere, which could not be determined with fresh olivine. The layer formation is considered by the authors to be caused by the intensive contact of bed material with burning char particles in the combustion reactor.

An unsolved problem of the plant in Güssing is the formation of fouling in the flue gas path after the combustion chamber. The main fouling that reduces the operation time significantly is located at the entrance of the first heat exchanger after the combustion chamber, which is an air preheater. It is a shell in a tube heat exchanger with the flue gas inside the tubes. The flue gas temperature at the entrance of the heat exchanger is around 830 °C, with wall temperatures of around 500 °C.

The influence of changing the ash loops on the behavior of the inorganic matter in the gasification system in terms of layer formation of the bed material and fouling and slagging is still unknown.

METHODS

The investigations of inorganic matters and their behavior in the system included analyses of the composition and amount of all flows for a qualitative evaluation of the possible behavior of the components. Balances of the main components of inorganic matter were determined to understand the influence of ash loops on the possible accumulation of substances in the system.

Sampling. Ash samples were taken during operation, and samples of fouling were taken during stops after cooling the plant. Fly ash samples (ash exiting the plant in the container, fine ash circulation, coarse ash circulation) were sieved with a vibratory sieve with 200 μm mesh size. The fraction smaller than 200 μm is defined as fine ash; the other fraction is defined as coarse ash.

The sampling points are shown in Figure 1 and described in Table 4. Mass flows that were not measured via the distributed control system (DCS) of the plant were measured manually, and three measurements were carried out over a period of 30 min.

Multiple samples of fouling were taken at the first heat exchanger (air preheater) of the flue gas after the combustion reactor.

dx.doi.org/10.1021/ef400598h | Energy Fuels 2013, 27, 3316−3331

Table 4. Sampling Points and Flow Determination[a]

sample type	sampling point no.	description	determination of flow
input flow	1	biomass ash	mass flow of biomass, ash content
input flow	2	bed material	level measurement DCS
input flow	3	precoat material	weight measurement DCS
internal flow	4	fly char	weight measurement DCS/ calculated after rebuild
internal flow	5	fine ash circulation	manual weight determination
internal flow	6	coarse ash circulation	manual weight determination
output flow	7	ash to container	manual weight determination
fouling	8	cyclone	
fouling	9	air preheater entry	
fouling	10	product gas cooler	(no analysis presented)

[a]Sampling point numbers are according to Figure 1.

Two different representative samples with different textures were presented as an example in this study.

Various samples of fouling in the cyclone were taken, and representative results are presented here. Due to the different appearance of the samples (see Figure 3), three different probes were analyzed: sample A was located at the surface of the fouling, sample B is material taken 3−4 mm below the surface, sample C was taken from the inner layer of the fouling close to the refractory lining.

Analyses. The elemental composition of the samples was determined using X-ray fluorescence (XRF) and calculated as oxides. Samples for XRF were melted in a Merck Spectromelt at 1050 °C and placed on a 400 °C stainless steel plate. The analyses were carried out with a PANalytical Axios Advanced analyzer under vacuum atmosphere with a rhodium anode, an excitation voltage of 50 kV, and a tube current of 50 mA. The results indicate the elemental composition of the total sample calculated in oxides.

Thermogravimetric analysis (TGA), differential thermal analysis (DTA), and differential scanning calorimetry (DSC) analysis were carried out in a NETZSCH STA 449 C Jupiter System. The sample crucible is equipped with a thermocouple for direct measurement of the temperature. The furnace allows temperatures of up to 1650 °C with heating rates of 0.01 to 50 K/min. A heating rate of 10 K/min was chosen. Gas used to provide the desired atmosphere flows upward and the desired gas composition is mixed from gas bottles of pure gases with the aid of mass flow controllers. The mass of each sample was chosen to be approximately 70 mg. Results of the DSC are indicated in microvolts, and calibration with $BaCO_3$ gave a calibration factor of 2.77, allowing the results to be obtained in milliwatts.

The TGA, DTA, and DSC analyses were carried out once for each sample but in three different atmospheres. Air, pure nitrogen as an inert gas, and a mixture of nitrogen with 15% CO_2 by volume were used as atmospheres to simulate reactions with the atmosphere such as combustion and calcination. The purge gas flow was set to 40×10^{-6} m^3/min. Due to the high inhomogeneity of the samples, a low repeatability of the analysis is expected but the authors expect to obtain only qualitative results, which will lead to qualitative conclusions about the operation of the system.

Mass Balances of Inorganic Matter. Ash flows were determined at different locations, shown in Table 4, for the preparation of the mass balances. The ash content was determined, and the elemental composition was measured by XRF and calculated in oxides. For the determination of the mass flows of the inorganic matter, the samples were calcined at 1050 °C to release carbonates and organic matter, and the mass flows are related to the calcined samples.

Mass balances of inorganic matter were calculated using the software STAN.[31] The software allows data reconciliation with the method of least-squares. The balances of inorganic matter are based on (a) the total balance of coarse and fine ash, (b) the elemental balance of CaO, MgO, SiO_2, Fe_2O_3, K_2O, and the sum of other elements for fine and coarse ash mass flows. The composition of bed material and precoat material was considered to be constant, and average values were taken. For the composition of biomass ash, an average composition was considered due to the high inhomogeneity of the fuel due to the utilization of different wood species, log sizes, and bark contents.

Various assumptions were made for the simplification of the system and are shown in Table 5. The bed material circulation mass flow between the gasifier and the combustion reactor was considered to be balanced and is not indicated in the balances because the mass flow of around 100 tons per hour is much higher than the other inorganic flows and would predominate over all other flows.

The standard deviation for the measured mass flows used is given in Table 6. Mass flows that are measured by DCS are considered to have a standard deviation of 2%, while manually measured mass flows are assumed to have a standard deviation of 10%. The abrasion is estimated from the coarse and fine ash balance and the standard deviation is chosen with 50% to be adjusted by the calculation method of the balance. Averages of analyses were obtained for the composition of biomass ash, precoat material, and bed material and the standard

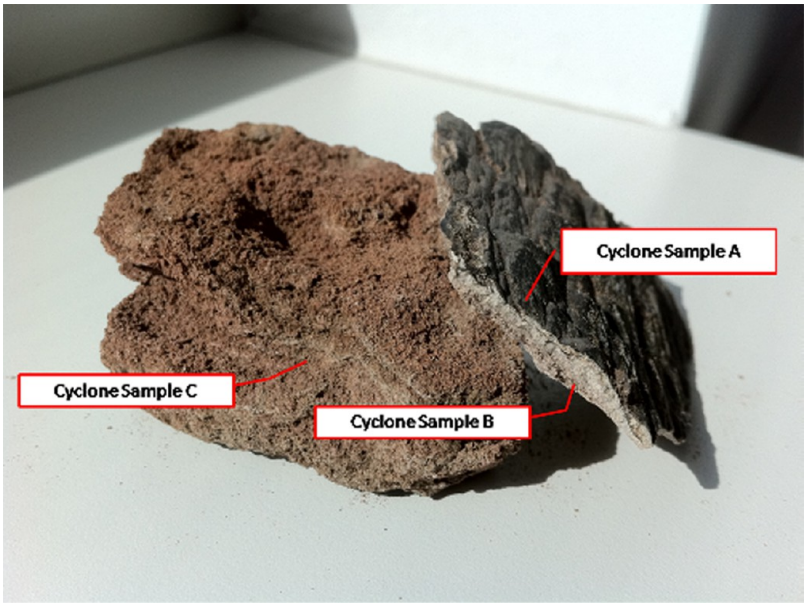

Figure 3. Sampling of fouling in the cyclone.

dx.doi.org/10.1021/ef400598h | Energy Fuels 2013, 27, 3316−3331

Table 5. Assumptions for the Mass Balance of the Inorganic Matter

- Mass flows of biomass ash, precoat material, fly char, and the mass flow from the combustion reactor to the gasifier were considered to have a particle size smaller than 200 μm.
- Bed material supplement and the flow from the gasification reactor to the combustion reactor are assumed to have a particle size bigger than 200 μm.
- The system is considered to be in a steady state condition, without accumulation of material in the system.
- Bed material circulation between the gasification reactor and the combustion reactor is considered to be balanced in terms of mass flow and composition. All variation of this balance is shown in the results. The balanced bed material circulation is not shown in the diagrams.
- Abrasion is the same in the combustion reactor as in the gasification reactor.
- Abraded material has the same composition as the fresh bed material.
- No inorganic matter is detectable in the gas after the product gas filter and the flue gas filter.

Table 6. Determination of the Mass Flows and Assumed Standard Deviations for the Mass Balances of Inorganic Matter

description	determination of flow	SD mass flow (%)	SD elemental composition (%)
biomass ash	mass flow of biomass, ash content	20	5
bed material	level meas. DCS	2	5
precoat material	wt meas. DCS	2	5
fly char	wt meas. DCS (calcd in Figure 9)	20	2
fine ash circulation	manual wt determination	10	2
coarse ash circulation	manual wt determination/wt meas. DCS	2	2
ash to container	manual wt determination	10	2
layer formation at the bed material	calcd	calcd	calcd
abrasion in combustion reactor	est.	50/calcd	5
abrasion in gasification reactor	est.	50/calcd	5

Table 7. Results of XRF for the Average Composition of Biomass Ash

	wood chip ash	
	avg (wt %)	SD (wt %)
Na_2O	2.77	2.66
MgO	5.13	0.45
Al_2O_3	2.57	1.10
SiO_2	15.36	7.52
P_2O_5	2.36	0.24
SO_3	1.26	0.51
K_2O	12.40	2.75
CaO	52.47	6.16
MnO	1.67	0.43
Fe_2O_3	1.73	0.66
Cl	0.42	0.36
others	1.85	
ash content (ds)	1.42	0.10

deviation of the composition of these mass flows was assumed to be 5%. Those analyses with specific analysis for the balance were considered to have 2% standard deviation.

Table 8. Typical Composition of the Precoat Material Dolomite

	precoat material (wt %)
Na_2O	2.32
MgO	32.01
Al_2O_3	1.36
SiO_2	1.48
P_2O_5	0.38
SO_3	0.44
K_2O	0.87
CaO	59.87
Fe_2O_3	0.63
Cl	0.30
others	0.35
loss on ignition 600 °C, 1 h	2.77%
loss on ignition 1050 °C, 1 h	44.66%

Table 9. Elemental Analysis of Olivine[10]

	olivine (wt %)
MgO	46.8
SiO_2	39.8
CaO	0.9
Fe_2O_3	10.3
K_2O	0.32
Na_2O	0.43
Al_2O_3	0.40
MnO	0.15
P_2O_5	0.03
Cl	0.10
SO_3	0.06
others	0.71

Table 10. Typical Composition of the Ash Entering the Container

	fine ash		coarse ash	
	avg. values (wt %)	SD (wt %)	avg. values (wt %)	SD (wt %)
Na_2O	1.19	1.00	1.20	0.92
MgO	19.67	2.06	37.27	2.61
Al_2O_3	1.52	0.90	0.52	0.21
SiO_2	20.28	8.97	35.70	4.00
P_2O_5	1.22	0.16	0.34	0.05
SO_3	0.39	0.22	0.08	0.03
K_2O	6.97	1.62	3.81	1.16
CaO	42.45	11.08	11.70	3.96
Fe_2O_3	4.08	1.60	8.01	0.58
Cl	0.26	0.17	0.19	0.13
others	1.96		1.19	
loss on ignition 600 °C, 1 h	4.94%		0.56%	
loss on ignition 1050 °C, 1 h	6.81%		1.05%	

Various balances were prepared, but two are presented that represent the status before the optimization project and the actual status. Before optimization, ash circulation is used (called "fine ash circulation" in Figure 1) where fly ash is circulated into the gasifier to minimize bed material consumption and to increase the amount of catalytic substances in the system. Coarse ash circulation was not implemented at the beginning of the project. During the optimization of the ash loops, a gravity separator was implemented in the system to separate bed material particles elutriated with the flue gas path from fly ash ("coarse ash circulation"). The second balance shows the status after the optimization project after the implementation of the coarse ash circulation and after turning off the fine ash circulation.

dx.doi.org/10.1021/ef400598h | Energy Fuels 2013, 27, 3316−3331

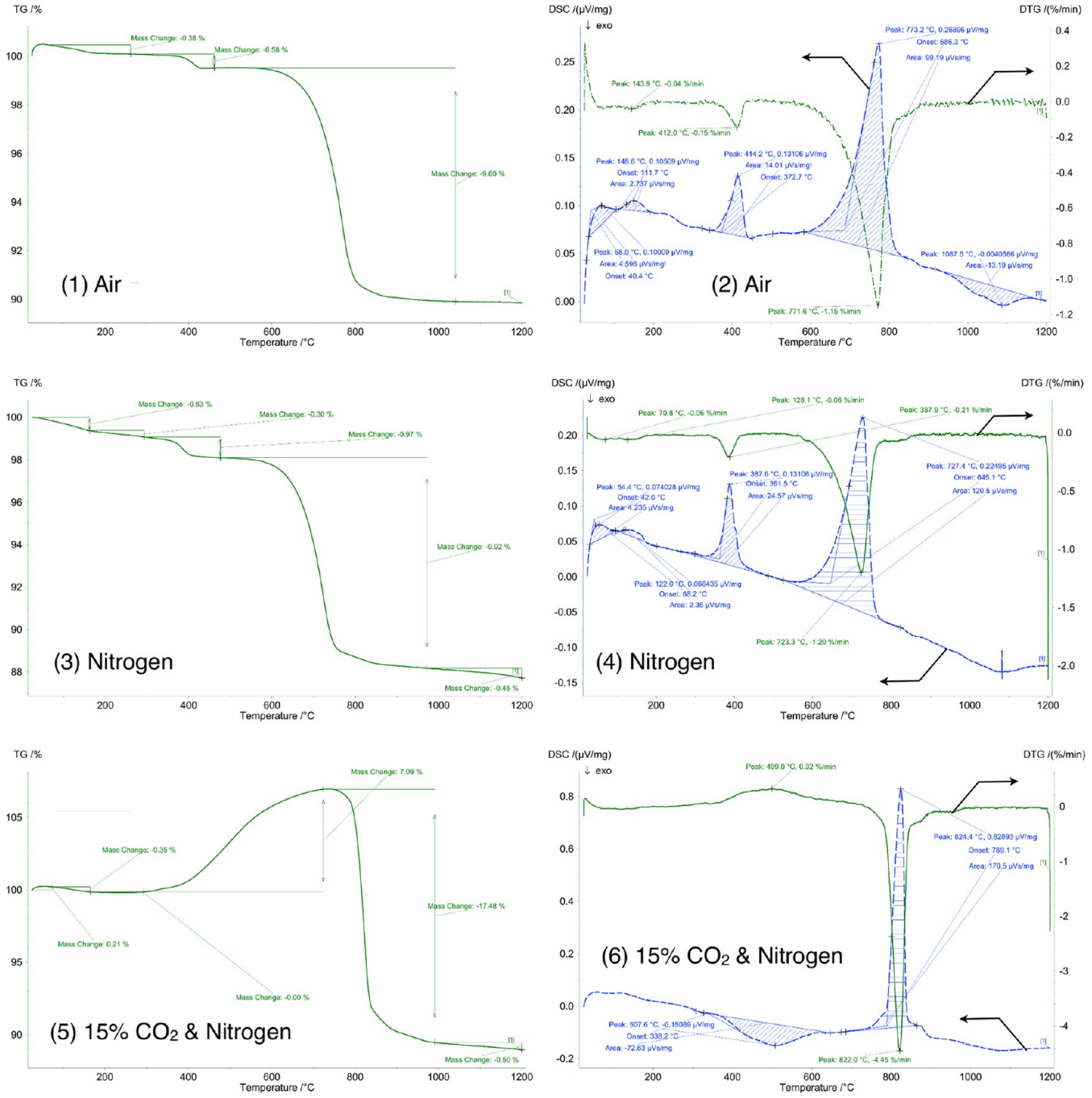

Figure 4. Thermal analysis of fly ash with particle size <200 μm in different atmospheres.

RESULTS

The composition of the biomass ash has a significant influence on fouling, slagging, and bed material agglomeration tendencies in the plant because it is the only source of components with low melting points. The quality of the biomass is constantly determined by the operational personnel in terms of water content but not ash content, bark content, or wood type. Table 7 shows the average biomass ash compositions and their standard deviations from samples taken in the years 2010 and 2011. The main component of the biomass ash is calcium oxide, which represents about half of the weight, followed by silicon oxide and potassium oxide. Magnesium oxide, phosphorus oxide, aluminum oxide, and sodium oxide are detectable in the low percentage range. The composition of the biomass ash is typical for hardwood ash as shown in literature.[32]

Precoat material is used for precoating the product gas filter and is added to the system. The precoat material described in Table 8 shows a typical composition of the natural mineral dolomite, whose main components are calcium and magnesium oxide, with a high ignition loss at 1050 °C, when the carbonates are released. Other elements are available in the low percentage range, such as sodium oxide, silicon oxide, and aluminum oxide.

The elemental composition of the olivine, which is used in the plant as a bed material, shows the main components magnesium oxide, silicon oxide, and iron oxide (Table 9). Other elements are available in low concentrations.

dx.doi.org/10.1021/ef400598h | *Energy Fuels* 2013, 27, 3316−3331

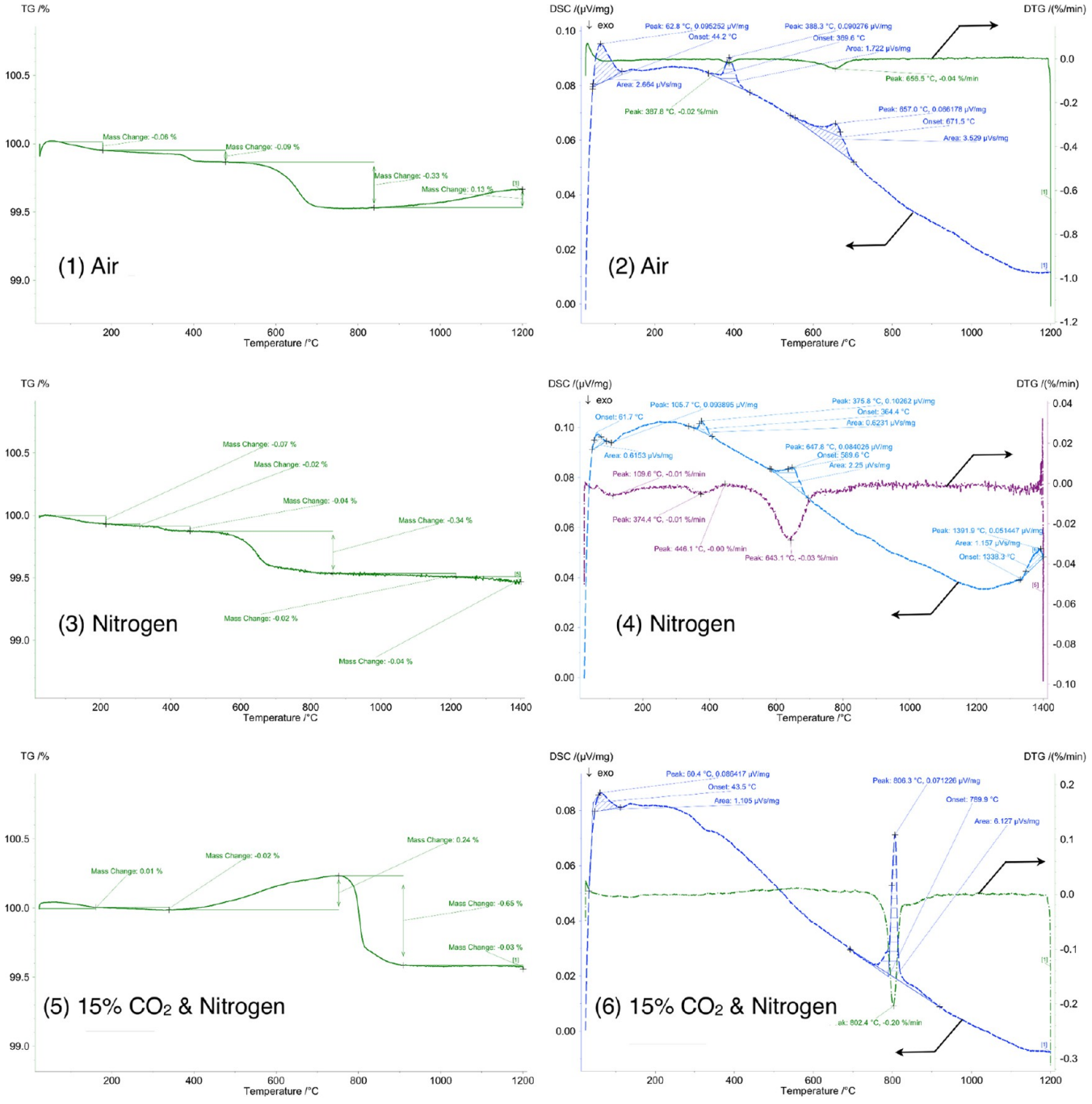

Figure 5. Thermal analysis of fly ash with particle size >200 μm in different atmospheres.

An overview of the composition of the fine ash (particles <200 μm) and coarse ash (particles >200 μm), which leave the process and enter the ash container, is shown in Table 10. Coarse ash consists of the main components of olivine, such as magnesium oxide, silicon oxide, and iron oxide, but also significant contents of calcium oxide (nearly 12 wt %) and potassium oxide (nearly 4 wt %), which originate from biomass ash. This is in agreement with the study presented earlier.[10] Fine ash mainly consists of calcium oxide, silicon oxide, magnesium oxide, and also potassium oxide. A high content of iron oxide is available, and other elements were detected such as sodium oxide, phosphorus oxide, and aluminum oxide. Important for the fouling tendency is the amount of potassium oxide, which is detectable in the fine ash, where it represents around 7 wt %, and in the coarse ash, where it represents only 4 wt %.

Table 11. Analysis of the fly Char before Optimization of the Ash Loops

		dry base	raw
water content	wt %		0.91
carbon content	wt %	26.14	25.9
hydrogen content	wt %	0.48	0.48
nitrogen content	wt %	0.06	0.06
ash content (db)	wt %	73.32	
upper heating value	kJ/kg	8301	8225
lower heating value	kJ/kg	8196	8097

dx.doi.org/10.1021/ef400598h | Energy Fuels 2013, 27, 3316−3331

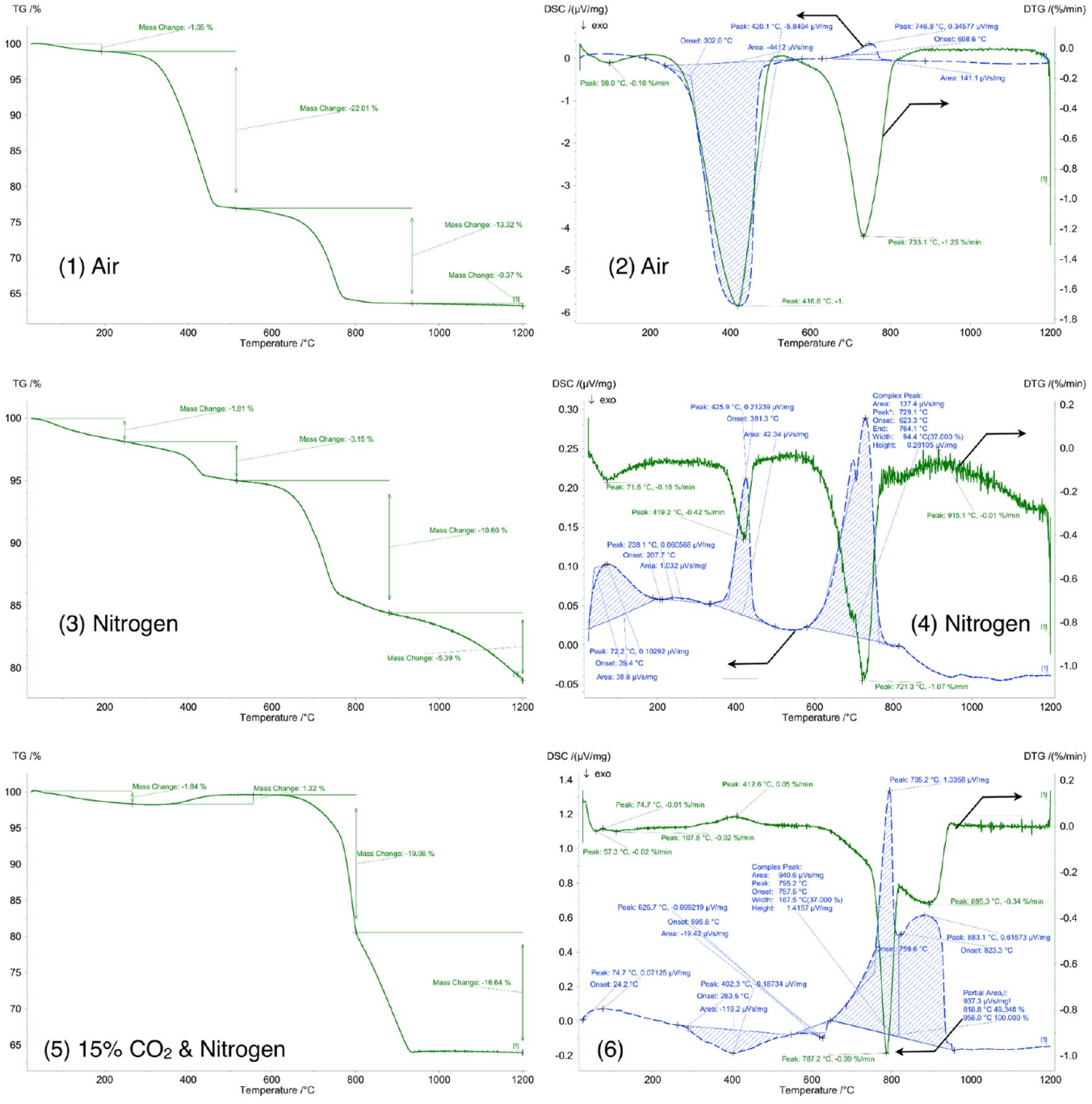

Figure 6. Thermal analysis of fly char in different atmospheres.

The thermal behavior of the fine fraction of fly ash in different atmospheres is shown in Figure 4. Two main peaks can be seen up to 1200 °C. At temperatures lower than 100 °C, small changes in weight are detectable. A weight loss with an endothermic signal in the DSC at around 400 °C and a significant endothermic weight loss at temperatures of around 720 to 820 °C are detectable. The results in air and nitrogen are similar; a significant change can be seen in the mixture of nitrogen with 15% CO_2. In a CO_2-rich atmosphere, an endothermic weight loss at 400 °C is not indicated but an increase in weight can be seen at temperatures higher than 400 °C with a strong endothermic peak at 820 °C.

The weight loss at temperatures around 100 °C is considered to be caused by the evaporation of water. An endothermic peak with weight loss at around 400 °C, which is not seen in the CO_2-rich atmosphere, is considered to be due to the calcination of magnesium carbonate. In the CO_2-rich atmosphere this is interfered by the adsorption of CO_2 on calcium oxide, which can be seen from the increase in the weight. Decomposition of calcium hydroxide is not considered at temperatures around 400 °C because it is expected at temperatures around 550 °C. The combustion and decomposition of organic matter (unburned wood) are not considered to happen because a peak can also be seen in the nitrogen atmosphere.

The thermal analysis of the coarse ash fraction of the fly ash shows properties similar to those of the fine ash but less pronounced (Figure 5). In contrast to the fine ash, an increase in weight can be seen at temperatures higher than 900 °C.

dx.doi.org/10.1021/ef400598h | Energy Fuels 2013, 27, 3316−3331

The weight loss of the fine ash fraction is around 10% while that of the coarse ash fraction is around 0.5%.

Coarse fly ash is considered to consist mainly of bed material, which is confirmed by the iron content. An increase in weight in the thermal analysis at temperatures higher than 900 °C might be caused by the oxidation of magnetite[33] or by the decomposition of fayalite with the oxidation of iron.

The investigations of the properties of the fly char include a fuel analysis because of the high carbon content of the char. The fuel analysis is shown in Table 11 and reveals that the fly char consists mainly of ash and carbon. The heating value justifies the utilization of the fly char as a fuel in the combustion reactor. The elemental analysis shown in Table 12 reveals the highest concentrations of the substances calcium oxide, magnesium oxide, silicon oxide potassium oxide, and iron oxide.

Table 12. Elemental Analysis of Inorganic Matter of Fly Char[a]

	mean value (wt %)	SD
Na_2O	1.94	1.36
MgO	25.02	2.83
Al_2O_3	2.38	0.63
SiO_2	22.13	2.17
P_2O_5	1.18	0.22
SO_3	0.38	0.26
K_2O	6.09	0.94
CaO	33.11	5.95
Fe_2O_3	5.24	0.19
Cl	0.52	n/a
others	2.0	
loss on ignition 1050 °C, 1 h	36%	

[a]Sample date, 2010.

The thermal analysis of fly char in different gas atmospheres (Figure 6) shows two significant endothermic peaks in air and nitrogen atmosphere at around 417 °C and around 730 °C. A low weight loss can be detected at temperatures up to 100 °C. In a mixture of 15% CO_2 in nitrogen, an exothermic peak can be seen at temperatures around 412 °C and a complex endothermic weight loss can be seen at temperatures between 795 and 880 °C.

The thermal analysis of the fly char showed combustion in air (exothermic peak) at 400 °C. In nitrogen atmosphere an endothermic weight loss can be seen at around 400 °C, which is considered to be due to the decomposition of magnesium carbonate. The low amount of oxygen in the char excludes the pyrolysis of organic matter, which could be also expected at this temperature. The endothermic weight loss at around 730 °C in the air and nitrogen atmosphere is considered to be caused by the decomposition of calcium carbonate and dolomite.[34] This reaction interferes in the CO_2-rich atmosphere with the CO_2-gasification of carbon with the peak at 880 °C.

The nature of fouling at the air preheater varies. The texture of the fouling varies from powder debris to hard and rocky material, which is difficult to remove. Soft and hard layers can be observed within one position but also at different locations. Due to the need for high availability of the plant, the inspection intervals for the heat exchanger are around four weeks and an exact determination of the formation of the fouling is not possible. The results of analyses of two different samples with different textures are shown in Table 13. Fouling that disaggregates easily to a powder has calcium oxide as its main component, accounting for nearly half of the mass of the sample. Magnesium and silicon oxide are detectable in about the same amount. The hard and rocky fouling shows a higher magnesium oxide concentration and lower calcium oxide and silicon oxide concentrations. Potassium oxide is significantly more highly concentrated in hard fouling, where it represents around 9 wt %, compared to 3.4 wt % in soft fouling.

Table 13. Elemental Analysis of Fouling at the Air Preheater

sample date	Oct. 3, 2010	Sept. 7, 2010
description	hard fouling at air preheater—untreated	fouling at air preheater that disaggregates easily
component	wt %	wt %
Na_2O	1.17	1.22
MgO	25.89	18.37
Al_2O_3	1.28	2.31
SiO_2	16.72	18.91
P_2O_5	1.68	1.92
SO_3	0.18	0.21
K_2O	9.15	3.40
CaO	36.29	47.81
Fe_2O_3	4.81	4.12
Cl	0.18	0.22
others	2.67	1.48
loss on ignition 1050 °C, 1 h	13.94%	3.71%

The thermal analysis of the fouling shown in Figure 7 gave different results compared to coarse ash and fine ash. The TGA shows a constant and significant weight loss of 8 to 10 wt % up to 1200 °C. The weight loss can be seen over the whole temperature range but increases at temperatures higher than 800 °C, and this is independent from the gaseous atmosphere. The DSC signal shows various endothermic peaks. Significant endothermic weight losses can be determined at around 100 °C, at 509 °C in air (526 °C in nitrogen and 532 °C in CO_2–nitrogen respectively), around 755 to 791 °C depending on the atmosphere, 864 to 978 °C, and above 1000 °C.

The first peak of the thermal analysis of the fouling occurs at temperatures around 100 °C, which is considered to be caused by evaporation of water. A significant peak can be observed at 509–530 °C, which is similar to the temperature at which the recrystallization of $K_2O{\cdot}SiO_2$[35] takes place and the similar temperature at which α-quartz is modified to β-quartz (573 °C).[36]

A peak at 755–791 °C with a high weight loss in air and nitrogen atmosphere and a moderate weight loss in CO_2-rich atmosphere might be caused by the decomposition of dolomite, calcium carbonate, or spurrite.[37−39] In the CO_2-rich atmosphere, this peak can be seen at 791 °C but the peak at 879 °C has a significantly higher weight loss. A high partial pressure of CO_2 can shift the decomposition of carbonates ($CaCO_3$ or spurrite) to higher temperatures. An overlapping of different reactions is suggested, where released CO_2 reacts with another component and is only released at higher temperatures. At temperatures between 864 and 878 °C, a recrystallization of quartz in β-tridymite[40] without weight loss is expected. Arvelakis et al.[38] showed that a mixture of K_2CO_3 and SiO_2 reacts to form potassium silicates at this temperature, leading to a weight loss because of the released carbonates.

In the nitrogen and CO_2-rich atmosphere, significant decomposition and melting can be seen (endothermic DSC signal with a weight loss), which agrees with the findings of Arvelakis et al.[38] that at temperatures higher than 1000 °C excessive decomposition and release in the gas phase of potassium rich compounds (KCl, K_2CO_3, K_2SO_4) as KOH are occurring.

dx.doi.org/10.1021/ef400598h | Energy Fuels 2013, 27, 3316–3331

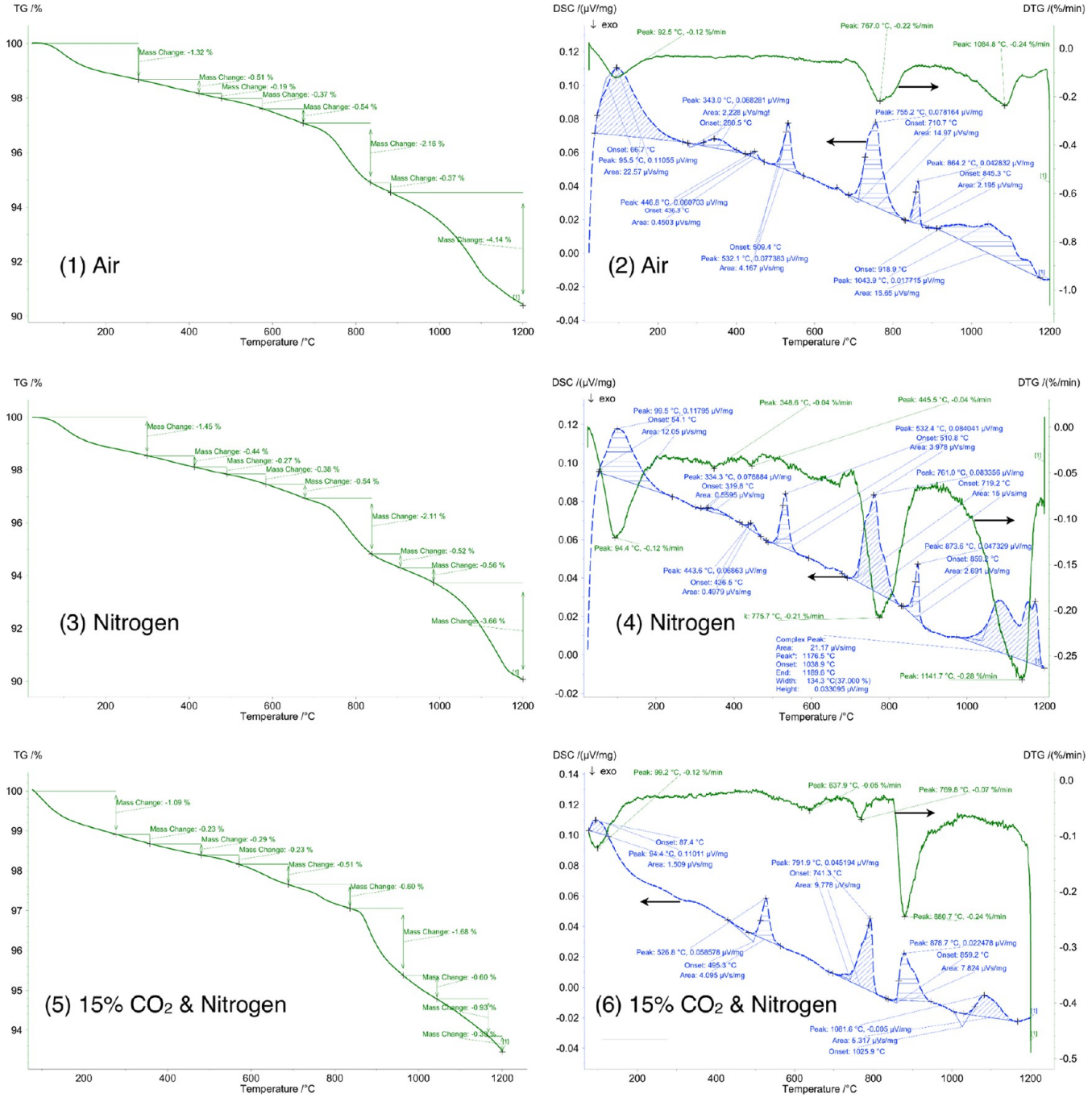

Figure 7. Thermal analyses of fouling at the air preheater in different atmospheres.

The results of the elemental composition of the fouling in the cyclone are shown in Table 14. The elemental analysis confirms the visual impression of the inhomogeneity of the fouling over its thickness. Bed material particles can be visually detected in sample C, which is confirmed by the high iron content of the sample. The amount of potassium in samples A and B, 23.6 and 19.1%, respectively, is significantly higher than is expected from the biomass ash. Calcium oxide content is lower in all samples compared to biomass ash.

Ash Balances. The ash balances were carried out for different operation modes of the ash loops. The status at the beginning of the optimization project is shown in Figure 8. A high amount of ash (coarse and fine) is circulated back into the gasifier before being released into the container to reduce bed material consumption and to increase the amount of catalytic substances in the system. It can be seen that this circulation of fine ash and coarse ash increases the total amount of ash in the system significantly. Considering that potassium is assumed to be responsible for fouling, the total input and output, respectively, from the system is 2.6 kg/h, while the potassium flow in the fly char is 16.8 kg/h. A significant amount of potassium is transferred from the combustion reactor to the gasification reactor via the siphon.

The status after the optimization of the ash loops is shown in Figure 9. The coarse ash circulation is fed into the combustion reactor while the fine ash circulation is turned off and all fine ash is released into the container. A significant reduction of the fine ash in the system can be seen. The amount of potassium

dx.doi.org/10.1021/ef400598h | Energy Fuels 2013, 27, 3316−3331

Table 14. Elemental Composition of the Fouling in the Cyclone (Main Components)

	cyclone sample A total sample (wt %)	cyclone sample B total sample (wt %)	cyclone sample C total sample (wt %)
Na_2O	0.53	0.35	2.88
MgO	11.09	14.82	28.51
Al_2O_3	1.22	2.51	0.89
SiO_2	25.84	29.34	36.84
P_2O_5	0.75	0.96	0.30
SO_3	0.13	0.03	0.06
K_2O	23.63	19.13	9.98
CaO	33.13	27.88	13.07
Fe_2O_3	2.36	3.42	6.03
Cl	0.08	0.06	0.44
others	1.26	1.50	0.99

that is transferred between combustion reactor and gasification reactor is reduced to 1.6 kg/h, which is around half of the amount of potassium that enters the plant with the biomass.

DISCUSSION

Discussion of Analyses of Inorganic Matter. The elemental analysis of biomass ash, precoat material (dolomite), and bed material did not reveal unexpected results. Combustion plants using alternative fuels such as straw and energy plants with high concentrations of chlorine, phosphor, and sulfur often show a fouling tendency.[29,41,42] These elements are detectable only in low concentrations in this study and are not considered to be the main reason for fouling in this case.

The reason is considered to be the interactivity between the inorganic flows that enter the plant: biomass ash, precoat material, and bed material. The influence of the interaction with the bed material was discussed and presented in earlier studies.[10−12] The tendency for fouling shows that interaction between biomass ash, abrasion of the bed material, and precoat material is happening. A comparison of the composition of the coarse fraction of the fly ash with used bed material[10] shows that the coarse fraction of the fly ash mainly consists of bed material.

The potassium content, which is considered to be responsible for fouling tendencies, is nearly doubled in the fine fly ash compared to coarse fly ash. The origin of potassium oxide is mainly the biomass ash.

The fuel analysis and elemental analyses of the fly char did not show unexpected results. The elemental composition of the inorganic fraction of fly char is similar to the fine fraction of the fly ash. Mass balances showed that the concentration of potassium in the fly char is higher than would be expected from the biomass ash.

The carbon in the fly char is considered to be bound closely to the ash due to the concentration of the ash component and condensation of gaseous inorganic species while cooling the product gas. According to the mechanism and modification of potassium of van Lith et al.,[25] potassium is available in organic species such as organic acids or bound on phenols.

Considering the elemental composition of the fouling at the air preheater, a high concentration of potassium and also calcium oxide and magnesium oxide can be seen. Fouling after fast fluidized bed combustion is described in the literature with a higher concentration of alkaline and alkaline earth metals compared to the composition of the biomass,[43] which can also be seen in this study. The difference in potassium content between loose agglomerates of ash and hard fouling at the air preheater is significant. The difference in the morphology of the fouling might be caused by variations of the operation conditions in the plant. High variation of the fuel water content between 20 and 40% causes variations in the operation of the combustion chamber such as temperature, oxygen concentration, and retention time.

The assumption that potassium is responsible for fouling is confirmed by the elemental analyses of the fouling in the cyclone. The surface of the fouling has a potassium concentration of around 24% by weight. Samples from the inside of the fouling and closer to the refractory lining showed lower concentrations of potassium oxide but higher concentrations of silicon oxide and magnesium oxide. The amount of calcium decreases on the inside of the fouling. Operational experience showed that the fouling formed rapidly within three days, which can be seen from the amount of bed material that leaves the cyclone with the flue gas. Operation of the plant is still possible for some weeks after the formation of fouling in the cyclone. The growth of the fouling is expected to be lower during this period, which explains the high potassium content at the surface of the fouling.

Thermal analyses of fly ash (coarse and fine) and fly char were similar except for the high carbon content of fly char, which combusts in an air atmosphere and is gasified in a CO_2-rich atmosphere at temperatures higher than 800 °C. Thermal analyses of fouling showed a high weight loss and a complex behavior. Due to the long retention time at the tube sheet of the heat exchanger, slow reactions are expected, which can cause recrystallization.

The analyses of the inorganic matter are only snapshots of conditions that can occur in the system. The standard deviation of the fuel ash analysis shows high variation in the ash composition of the fuel. This is evident because biomass is bought from various fuel suppliers and the wood yard management is mainly based on the fuel water content. These single analyses are not sufficient to draw conclusions about the behavior of the inorganic matter in the system, and mass balances of inorganic matter need to be considered.

Discussion of Mass Balances of Inorganic Matter. The ash balances showed that the circulation of ash and the setup of the loops can lead to the transportation of ash through the reactors in amounts many times higher than the amount of inorganic matter, which is introduced into the system. This can lead to an accumulation of different substances within the system. Considering the potassium balances, a transfer of potassium from the combustion reactor to the gasification reactor can be detected in all the balances. This transfer leads to potassium concentrations in the fly char that are higher than expected with the mixture of abraded bed material and precoat material. The fly char also consists of unconverted char, which is mainly carbon. According to the findings of Novaković et al.,[26] potassium is released to the gas phase, which is enhanced by the presence of water, calcium oxide, and high temperatures. The release of potassium is also pronounced in gasification atmospheres.[27,28] Based on this knowledge, a close connection between potassium that is released to the gas phase and char can be expected due to the condensation processes of gaseous potassium during cooling of the product gas.

During combustion of fly char in the combustion reactor, the high carbon content of the char (see Table 11) leads to high combustion temperatures, which are responsible for the release of potassium into the gas phase. Scala et al.[44] showed

dx.doi.org/10.1021/ef400598h | Energy Fuels 2013, 27, 3316−3331

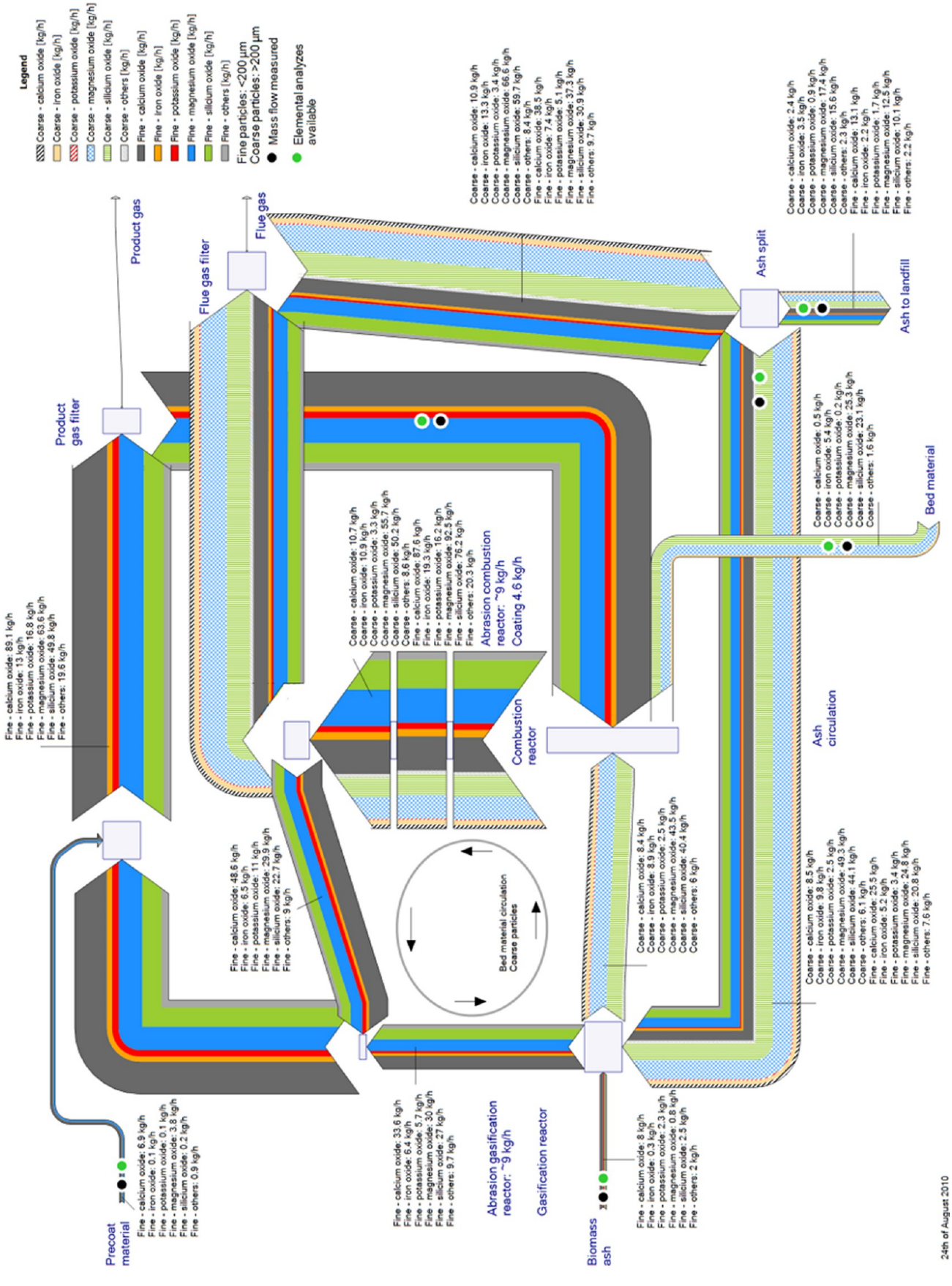

Figure 8. Mass balance of inorganic matter before optimization.

dx.doi.org/10.1021/ef400598h | *Energy Fuels* 2013, 27, 3316−3331

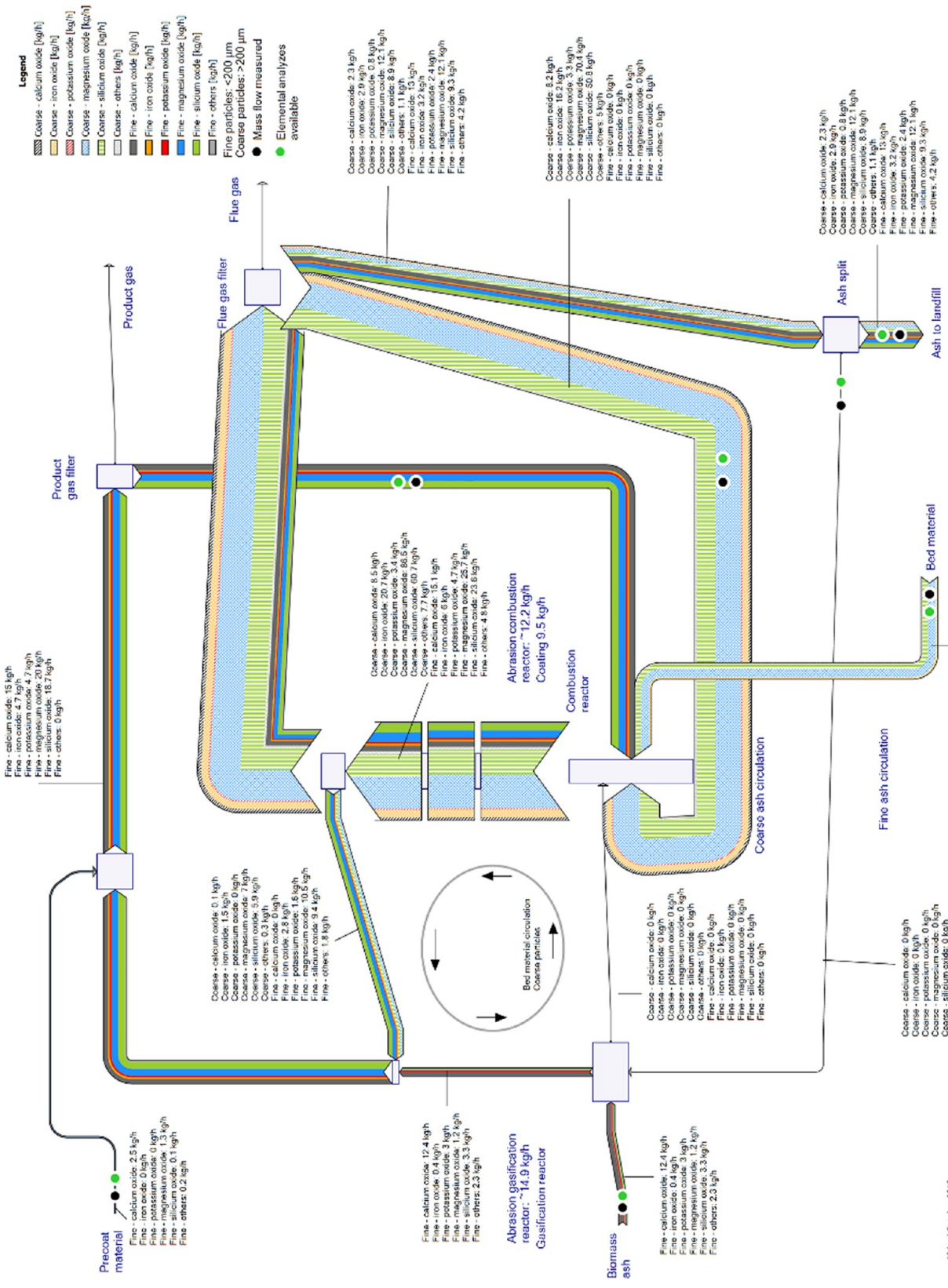

Figure 9. Mass balance of inorganic matter with coarse ash circulation into the combustion reactor and fine ash turned off.

dx.doi.org/10.1021/ef400598h | *Energy Fuels* 2013, 27, 3316−3331

that agglomeration takes place around burning char particles because their temperature is the highest temperature in the fluidized bed.

Low potassium release rates can be achieved by low temperatures, low water content in the combustion reactor, and low calcium content in the system. The temperatures are linked to the demand for a proper gasification temperature and also the bed material circulation rate between the gasification and combustion reactors and the excess air ratio in the combustion reactor. Keeping the excess air ratio in the combustion chamber high will decrease the adiabatic combustion temperature of the burning char particles and reduce the potassium release rate.

The mechanism for the transfer of potassium from the combustion reactor to the gasification reactor is unknown. Different possibilities are suggested: (a) Due to the higher release rate of potassium in the combustion reactor, the potassium concentration in the bed material particles is increased and potassium is released in the gasification reactor. Gaseous potassium is considered to be available in cavities of the bed material.[10] (b) The release rate of potassium is higher in the gasification reactor due to the reducing atmosphere. The fraction of potassium that is bound to the bed material is higher in the combustion reactor compared to the gasification reactor. This can be in the form of potassium carbonate (liquid or solid) in the combustion reactor, which is reduced to potassium hydroxide in the gasification reactor. (c) A higher temperature and the oxidizing conditions in the combustion reactor lead to partly melting silicates that are attached to the bed material and transferred with the bed material into the gasification reactor, where potassium is released to the gas phase.

Sampling of bed material in the combustion chamber and the gasifier is not possible due to high temperatures. The difference in potassium concentration in the bed material between combustion reactor and gasifier can be considered to be below the detection limit of the analysis. Further investigations are required to clarify the mechanism of the overflow of potassium between combustion reactor and gasification reactor.

CONCLUSION

The following conclusions can be drawn from the analyses and balances of inorganic matters in the DFB plant presented in this paper:

- Ash loops can lead to significantly higher material streams and to an accumulation of substances with low melting points in the system.
- Potassium, which is considered to be mainly responsible for fouling, slagging, and bed material agglomeration in this case, is transferred from the combustion reactor to the gasification reactor. The mechanism of the transfer is still unknown.
- An accumulation of potassium can be seen in the fly char.
- The concentration of potassium in fine ash is nearly twice that in the coarse ash and bed material.

For the operation of the DFB plants, the following recommendations are given:

- A reduction of potassium in the system can be achieved by consequent and immediate discharge of fine ash. Recirculation of fine ash should be avoided.
- The melting behavior of ashes and the catalytic activity of the bed material are influenced significantly by the inorganic loops. Accurate measurement and control of ash and bed material streams are recommended.
- The high concentration of inorganic matter in the fly char, which is assumed to be closely bound to the char, demands accurate control of the fly char entering the combustion chamber as well as accurate control of the combustion air to avoid temperature variations and to keep the adiabatic combustion temperature of the particles as low as possible.
- A convective path for cooling the flue gas is recommended to cool inorganic matter before it comes into contact with a tube sheet of heat exchangers or tubes. It is also suggested that this may be useful while cooling the product gas.

AUTHOR INFORMATION

Corresponding Author

*Phone: + 43 (0) 3322 42606-156. Fax: + 43 (0) 3322 42606-199. E-mail: friedrich.kirnbauer@bioenergy2020.eu.

Notes

The authors declare no competing financial interest.

ACKNOWLEDGMENTS

This study was carried out in the frame of the Bioenergy2020+ project "C-II-1-7 Advanced biomass Steam Gasification". Bioenergy2020+ GmbH is funded within the Austrian COMET program, which is managed by the Austrian Research Promotion Agency (FFG). We are grateful for the support of our project partners Biomasse-Kraftwerk Güssing GmbH, Repotec Umwelttechnik GmbH, and the Institute of Chemical Engineering, Vienna University of Technology.

REFERENCES

(1) Valmari, T.; Lind, T. M.; Kauppinen, E. I.; Sfiris, G.; Nilsson, K.; Maenhaut, W. *Energy Fuels* **1998**, *13*, 379−389.

(2) Davidsson, K. O.; Amand, L. E.; Steenari, B. M.; Elled, A. L.; Eskilsson, D.; Leckner, B. *Chem. Eng. Sci.* **2008**, *63*, 5314−5329.

(3) *E4Tec. Review of Technologies for Gasification of Biomass and Wastes; NNFCC Publications Final Report*, 9th ed.; NNFCC: York, U.K., 2009; p 130.

(4) Hofbauer, H.; Rauch, R.; Loeffler, G.; Kaiser, S.; Fercher, E.; Tremmel, H. In *Proc. 12th European Conf. Biomass Bioenergy*, Amsterdam, The Netherlands, 2002; p 4.

(5) Kotik, J. *Über den Einsatz von Kraft-Wärme-Kopplungsanlagen auf Basis der Wirbelschicht-Dampfvergasung fester Biomasse am Beispiel des Biomassekraftwerks Oberwart*; Vienna University of Technology: Vienna, Austria, 2010 (in German).

(6) Klotz, T. A regional energy-supply-showcase—The 15 MW fuel-power biomass gasification plant Villach. *International Seminar on Gasification*, Gothenburg, 2010.

(7) SWU Stadtwerke Ulm/Neu-Ulm GmbH. *Strom und Wärme aus der Natur*; http://www.swu.de/fileadmin/Content/PDFs/Energie_Wasser/Web_Flyer_HGASenden_16032012.pdf (accessed March 8, 2013) (in German).

(8) Bolhar-Nordenkampf, M.; Hofbauer, H.; Bosch, K.; Rauch, R.; Aichernig, C. In *Proc. Int. Conf. Biomass Utilisation*, Phuket, Thailand, 2003; Vol. *1*, pp 567−572.

(9) Koppatz, S.; Pfeifer, C.; Rauch, R.; Hofbauer, H.; Marquard-Moellenstedt, T.; Specht, M. *Fuel Process. Technol.* **2009**, *90*, 914−921.

(10) Kirnbauer, F.; Hofbauer, H. *Energy Fuels* **2011**, *25*, 3793−3798.

(11) Kirnbauer, F.; Wilk, V.; Kitzler, H.; Kern, S.; Hofbauer, H. *Fuel* **2012**, *95*, 553−562.

(12) Kirnbauer, F.; Wilk, V.; Hofbauer, H. *Fuel* **2012**, *108*, 534−542.

(13) Hofbauer, H.; Rauch, R.; Bosch, K.; Koch, R.; Aichernig, C. In *Pyrolysis and Gasification of Biomass and Waste*; Bridgwater, A. V., Ed.; CPL Press: Newbury, Berks, U.K., 2003; pp 527−536.

(14) Pronobis, M. *Fuel* **2006**, *85*, 474−480.

(15) Plaza, P.; Griffiths, A. J.; Syred, N.; Rees-Gralton, T. *Energy Fuels* **2012**, *23*, 3437−3445.
(16) Teixeira, P.; Lopes, H.; Gulyurtlu, I.; Lapa, N.; Abelha, P. *Biomass Bioenergy* **2012**, *39*, 192−203.
(17) Valmari, T.; Lind, T. M.; Kauppinen, E. I.; Sfiris, G.; Nilsson, K.; Maenhaut, W. *Energy Fuels* **1998**, *13*, 390−395.
(18) Miles, T. R.; Baxter, L. L.; Bryers, R. W.; Jenkins, B. M.; Oden, L. L. *Biomass Bioenergy* **1996**, *10*, 125−138.
(19) Nielsen, H. P.; Baxter, L. L.; Sclippab, G.; Morey, C.; Frandsen, F. J.; Dam-Johansen, K. *Fuel* **2000**, *79*, 131−139.
(20) Miles, T. R.; Baxter, L.; Bryers, R. W.; Jenkins, B. M.; Oden, L. L. *Alkali Deposits Found in Biomass Power Plants*, NREL/TP-433-8142; NREL: Golden, CO, 1995.
(21) Boström, D.; Broström, M.; Skoglund, N.; Boman, C., Backman, R.; Öhman, M.; Grimm, A. *Ash Transformation Chemistry during Energy Conversion of Biomass*; LULEÅ University of Technology: Saariselkä, Lapland, Finland, 2010.
(22) Boström, D.; Skoglund, N.; Grimm, A.; Boman, C.; Öhman, M.; Broström, M.; Backman, R. *Energy Fuels* **2012**, *26*, 85−93.
(23) Kracek, F. C.; Bowen, N. L.; Morey, G. W. *J. Phys. Chem.* **1929**, *33*, 1857−1879.
(24) Scala, F.; Chirone, R. *Biomass Bioenergy* **2008**, *32*, 252−266.
(25) van Lith, S. C.; Jensen, P. A.; Frandsen, F. J.; Glarborg, P. *Energy Fuels* **2008**, *22*, 1598−1609.
(26) Novaković, A.; van Lith, S. C.; Frandsen, F. J.; Jensen, P. A.; Holgerson, L. B. *Energy Fuels* **2009**, *23* (7), 3423−3428.
(27) Sams, D. A.; Talverdian, T.; Shadman, F. *Fuel* **1985**, *64*, 1208−1214.
(28) Dayton, D. C.; French, R. J.; Milne, T. A. *Energy Fuels* **1995**, *9*, 855−865.
(29) Grimm, A.; Öhman, M.; Lindberg, T.; Fredriksson, A.; Boström, D. *Energy Fuels* **2012**, *26*, 4550−4559.
(30) Kirnbauer, F.; Hofbauer, H. *Powder Technol.* **2013**, *245*, 94−104.
(31) Cencic, O.; Rechberger, H. *J. Environ. Eng. Manage.* **2008**, *18*, 3−7.
(32) Vassilev, S. V.; Baxter, D.; Andersen, L. K.; Vassileva, C. G. *Fuel* **2010**, *89*, 913−933.
(33) Fredriksson, H. O. A.; Lancee, R. J.; Thüne, P. C.; Veringa, H. J.; Niemantsverdriet, J. W. H. *Appl. Catal., B* **2012**, 1−23.
(34) L'Vov, B. V. *Thermochim. Acta* **1997**, *303*, 161−170.
(35) Roedder, E. Silicate melt systems. *Phys. Chem. Earth* **1959**, *3*, 224−297.
(36) Bragg, W.; Gibbs, R. E. *Proc. R. Soc. A* **1925**, *109*, 405−427.
(37) Engler, P.; Santana, M. W.; Mittleman, M. L.; Balazs, D. *Thermochim. Acta* **1989**, *140*, 67−76.
(38) Arvelakis, S.; Jensen, P. A.; Dam-Johansen, K. *Energy Fuels* **2004**, *18*, 1066−1076.
(39) Goswami, G.; Padhy, B. P.; Panda, J. D. *J. Therm. Anal. Calorim.* **1989**, *35*, 1129−1136−1136.
(40) Kracek, F. C.; Brown, N. L.; Morey, G. W. *J. Phys. Chem.* **1937**, *41*, 1183−1193.
(41) Zintl, F.; Strömberg, B.; Björkman, E. *Biomass for Energy and Industry: 10th European Conference and Technology Exhibition, Proceedings of the International Conference*, Wuzburg, Germany, June 8−11, 1998; pp 8−11.
(42) De Geyter, S. *The role of sulphur in preventing bed agglomeration during combustion of biomass*. M.S. Thesis. Umeå University, Sweden, 2006
(43) Jenkins, B. M.; Baxter, L. L.; Miles, T. R. *Fuel Process. Technol.* **1998**, *54*, 17−46.
(44) Scala, F.; Chirone, R. *Energy Fuels* **2006**, *20*, 120−132.